Supporting Information

A Wearable Bipolar Rechargeable Aluminum Battery

Zejing Lin,[1,2] Minglei Mao, [1] Jinming Yue, [1] Binghang Liu, [1] Chuan Wu, [3] Liumin Suo, *[1 2 4] Yong-Sheng Hu, [1] Hong Li, [1] Xuejie Huang, [1] Liquan Chen[1]

[1]Key Laboratory for Renewable Energy, Beijing Key Laboratory for New Energy Materials and Devices

Institute of Physics, Chinese Academy of Sciences

Beijing, 100190, China

[2]Center of Materials Science and Optoelectronics Engineering

University of Chinese Academy of Sciences

Beijing, 100049, China

[3]Beijing Key Laboratory of Environmental Science and Engineering

School of Materials Science and Engineering, Beijing Institute of Technology

 Beijing, 100081, China

[4]Yangtze River Delta Physics Research Center Co. Ltd

Liyang, 213300, China

*Corresponding author e-mail: suoliumin@iphy.ac.cn

Contents

Experiment

Cell Assembly:

Electrolyte Preparation: $AlCl_3$: [EMIm]Cl (1.3:1) electrolyte was prepared by slowly adding anhydrous aluminum chloride ($AlCl_3$, 1.3 mole ratio, 99.999%, Acros) to 1-ethyl-3-methyl-imidazolium chloride ([EMIm]Cl, 99%, Shanghai Chengjie Ionic Liquid Company) under stirring in an argon atmosphere glove box (<0.1 ppm of water and oxygen). [EMIm]Cl was dried in the glove box at 130 °C overnight before use.

Cathode fabrication: KS6L/CPF cathode was prepared by pressing KS6L (SCM Hypnergy Material Tech Co., Ltd), ketjen black (Triquo Chemical) and PTFE (Alfa Aesar) at a weight ratio of 8:1:1 onto the CPF (Caplinq).

Anode fabrication: Al/CPF anode was prepared by stacking CPF, Al foil, separator (Whatman GF/A glass fiber) and polyethylene insulator frame in the sequence and heat-sealing all four edges by commercial hand heat sealer in the glove box. Aluminum foil (99.99%, Alfa Aesar) was polished in the glove box to remove the oxidation film before use.

Bipolar plate fabrication: KS6L/CPF/Al bipolar plate was prepared by heat sealing back side of KS6L/CPF, Al foil, separator (Whatman GF/A glass fiber) and polyethylene insulator frame together.

Assembly process: The M-RAB was prepared by heat-sealing three edges of one KS6L/CPF cathode and one Al/CPF anode to make a sealed bag. After adding $AlCl_3$: [EMIm]Cl electrolyte, another edge was sealed at 115 °C under vacuum by heat sealer (MTI, MSK-115A-S). 2-stacked B-RAB was prepared by heat-sealing one KS6L/CPF cathode, one KS6L/CPF/Al bipolar plate and one Al/CPF anode together as the above single one did. And 5-stacked B-RAB was stacked by one KS6L/CPF cathode, four KS6L/CPF/Al bipolar plates and one Al/CPF anode.

Electrochemistry measurements:

Linear sweep voltammetry (LSV) was performed using a three-electrode cell on CHI660E electrochemical workstation with aluminum foil, aluminum wire and investigated current collectors (Ta, Mo, Ni, SS, Ti, PG, CPF) as a counter electrode, a reference electrode and a working electrode respectively at a scan rate of 5 mV/s from 0.1 V to 2.8 V.

Cyclic voltammetry (CV) was carried out on M-RAB at a scan rate of 0.5 mV/s from 0.5 V to 2.3 V.

Galvanostatic tests were conducted on Neware battery test station.

Material Characterizations:

The morphology of the CPF and cross-section of KS6L/CPF cathode were investigated by scanning electron microscope (SEM, HITACHI, S4800).

Thermogravimetric (TG) and differential scanning calorimetry (DSC) curves of CPF were tested at a heating rate of 10 ℃ /min from room temperature to 800 ℃ in an air atmosphere (NETZSCH, STA 449C).

Calculation

To evaluate the influence of two different structures on the distance of current traveling, the simplified models of both conventional serial current collectors and bipolar current collectors are shown in Figure S1. L is the length of the current collector, d stands for its thickness and w represents its width.

In the conventional pack of cells connected in series (Figure S1a), current travels over the whole length of the current collector through the red cross-section area, the resistance from each conventional monopolar current collector (R_c) can be calculated using the following equation:

$$R_c = \rho \frac{L}{A} = \rho_c \frac{L}{w \cdot d}$$

In an actual serial pack, other resistances also exist unavoidably, such as the connect resistance between tab and current collector but to make a simple estimate of current collector resistivity, only the inner parts within the package are considered here. Thus, the whole resistance from the current collectors of a conventional pack (R_{cp}) with several monopolar cells in series can be calculated as:

$$R_{cp} = n \cdot 2 \cdot R_c = \rho_c \frac{2n}{w} \cdot \frac{L}{d}$$

While in the bipolar pack, current flows across the thickness of the current collector through the blue area, the resistance from each bipolar current collector (R_b) is calculated as:

$$R_b = \rho \frac{L}{A} = \rho_b \frac{d}{w \cdot L}$$

And the whole resistance from current collectors of a bipolar pack (R_{bp}) with several cell stacked can be expressed with the following equation:

$$R_{bp} = (n + 1) \cdot R_b = \rho_b \frac{(n+1)}{w} \cdot \frac{d}{L}$$

When the same current collectors are adopted, since the value of L (centimeter-scale) is much bigger than that of d (micron-scale), the value of L/d is also bigger than that of d/L, leading to the much smaller R_{bp} than R_{cp}.

In another way, when the resistance generated in the bipolar pack is the same as conventional one did, the resistivity of bipolar current collector can be expanded as follows:

$$R_{bp} = R_{cp}$$

$$\rho_b \frac{(n+1) \cdot d}{w \cdot L} = \rho_c \frac{2n \cdot L}{w \cdot d}$$

$$\frac{\rho_b}{\rho_c} = \frac{2n}{n+1} \cdot \left(\frac{L}{d}\right)^2$$

For example, for a conventional pouch pack of two serial cells cell with a size of 10-cm-length and 25-μm-thick current collector, the value of ρ_b can be expanded seven orders of magnitude larger than ρ_c. The resistivity of commonly applied aluminum foil current collector in lithium-ion batteries is $2.8 \times 10^{-8}\,\Omega\cdot m$, which means any current collector with resistivity below $2.8 \times 10^{-1}\,\Omega\cdot m$ can be accepted in bipolar cells. The resistivity of reported current collectors are summarized in Table S1, limited by the current products, $1.8 \times 10^{-2}\,\Omega\cdot m$ is the minimum value of CPF reaching, but it can be applied in the bipolar structure according to the above calculation.
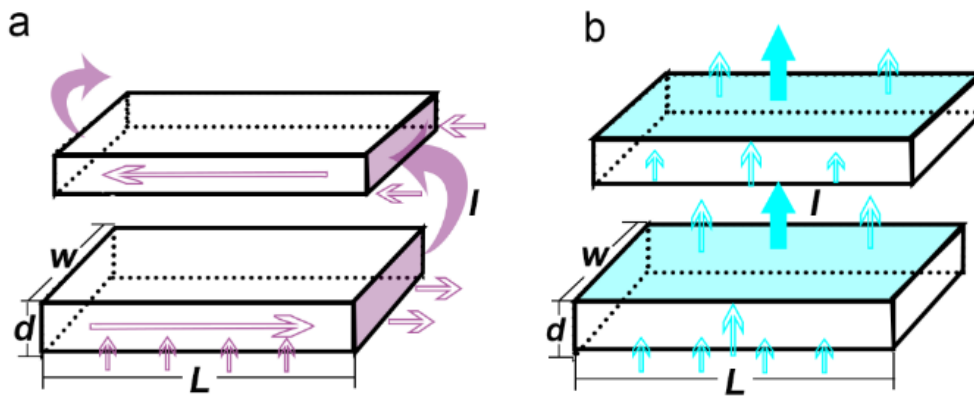
Figure S1. Simplified schematic of current collectors and current transfer path in (a) conventional pack and (b) bipolar pack.

Table S1. Resistivity and cost of current collectors

	Current collectors	Thickness (μm)	Resistivity (Ω·m)	Density (g/cm^3)	Weight (mg/cm^2)	Cost ($/m^2)
Reported in RABs	Ta	25	1.35×10^{-7}	16.6	41.5	255
	Mo	25	5.6×10^{-8}	10.2	25.5	49
	Ni	25	7.0×10^{-8}	8.9	22.3	7.8
	SS	25	7.4×10^{-7}	8.1	20.3	1.6
	Ti	25	4.2×10^{-7}	4.5	11.3	6.2
	PG	50	1×10^{-6}	2.1	10.5	10.5
This work	CPF	90	1.8×10^{-2}	1.18	10.6	2.9

SS: 316L stainless steel; PG: Pyrolytic graphite; CPF: Carbon black/polyethylene composite film

The pricing data of Ta and Mo current collector came from Alibaba.com and the data of CPF came from Caplinq.com, while others were referenced in previous studies[1, 2].
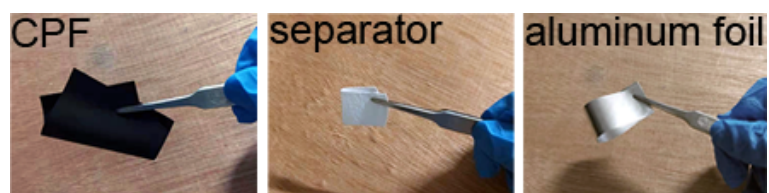
Figure S2. The optical pictures of flexible components of B-RAB including CPF, separator and Aluminum foil.
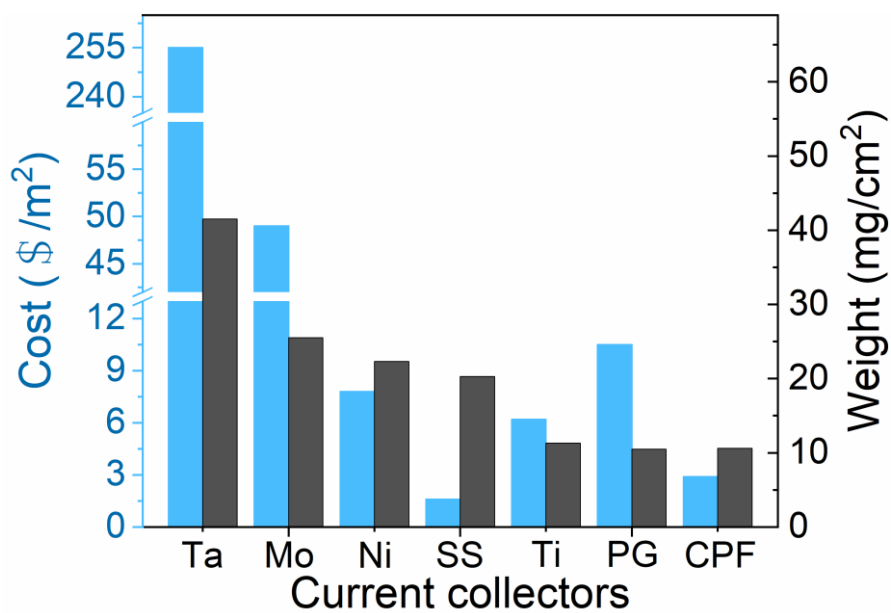
Figure S3. The cost and weight comparison of current collectors.

Compared with other metal current collectors, carbon-based CPF possesses the lowest weight with a relatively lower price, which is much favorable for portable electronics.
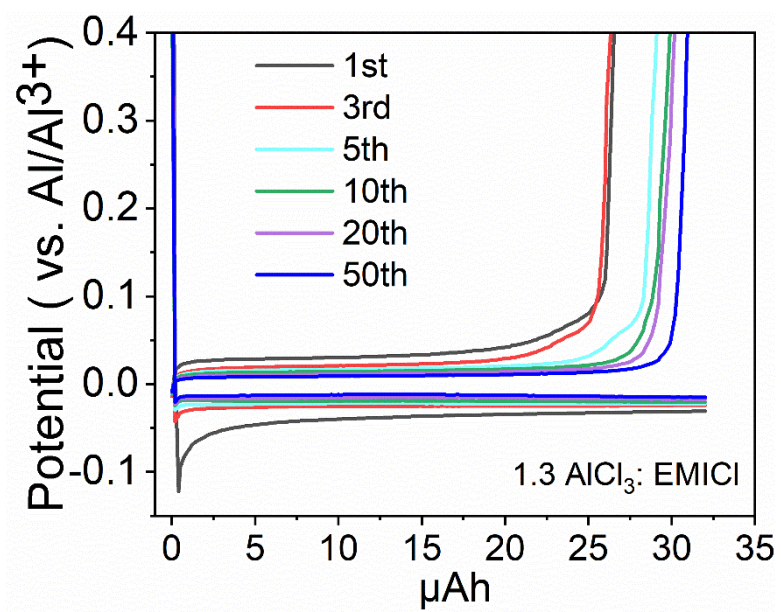
Figure S4. The aluminum deposition/striping in the prepared AlCl$_3$: [EMIm]Cl (1.3:1) electrolyte.

Assembly of M-RAB
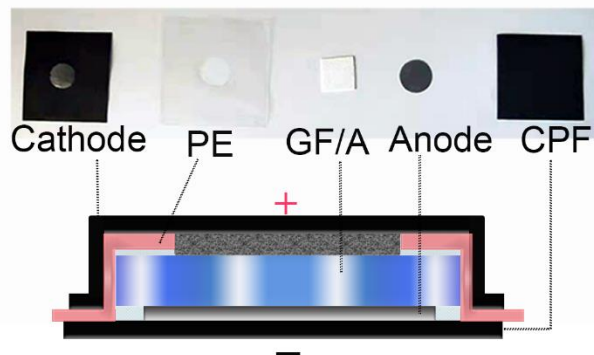
step 1 *KS6L/CPF Cathode*

step 2 *Al/CPF Anode*

step 3 *M-RAB*

step 4 *OCV of M-RAB and running a timer*

Figure S5. Assembly process and application of M-RAB with CPF serving as the current collector, cell case, and encapsulant.
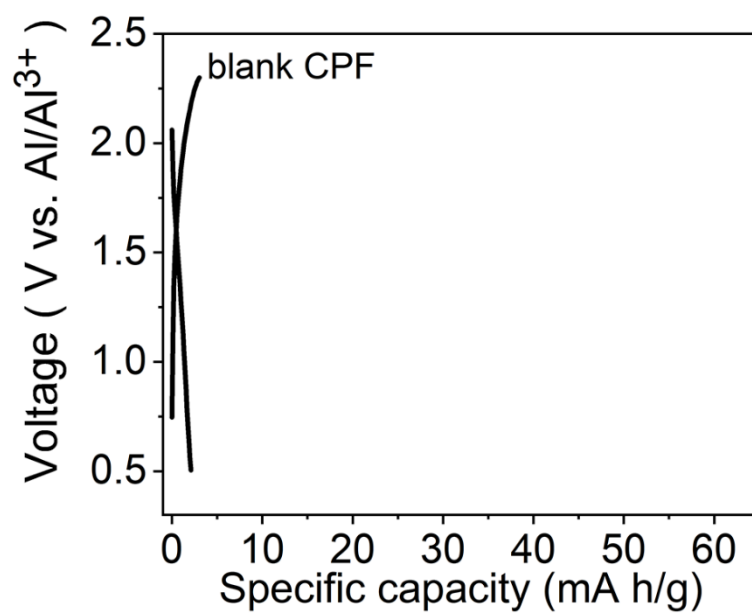
Figure S6. Charge and discharge curves of M-RAB without cathode materials.

 Few capacities can be observed in the battery, indicating that active $AlCl_4^-$ and $Al_2Cl_7^-$ can not react with the CPF components.
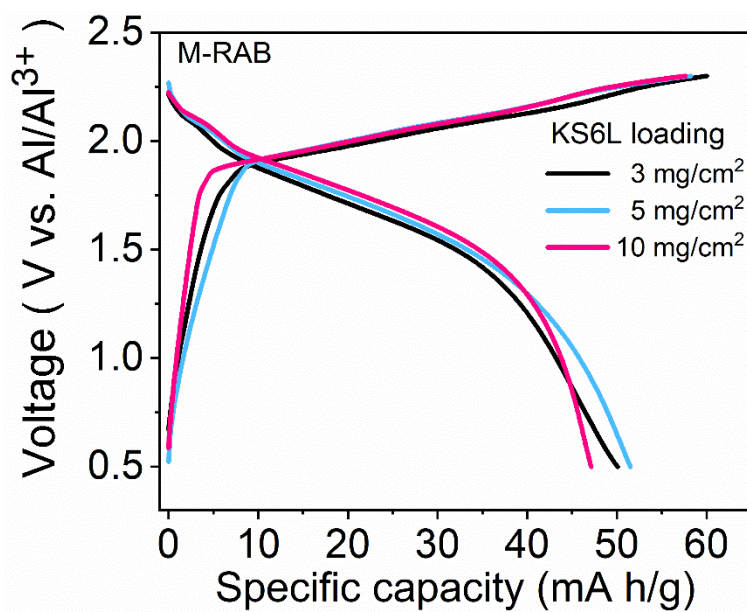
Figure S7. Charge and discharge curves of M-RAB at different mass loading.

The charge-discharge curves of M-RAB display a similar platform and discharge capacity as the mass loading of KS6L increasing from 3 to 10 mg, showing the small polarization of M-RAB.
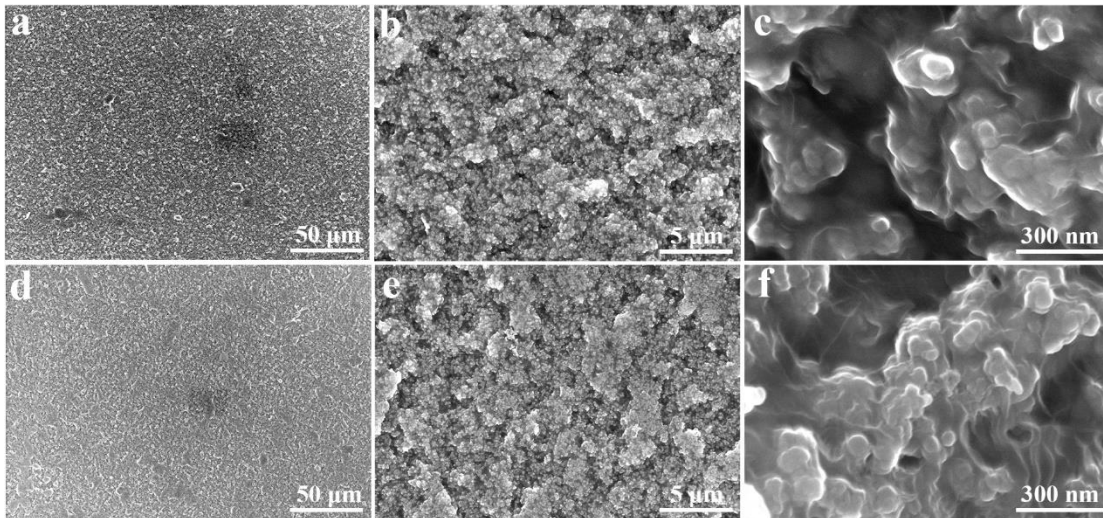
Figure S8. SEM micrographs of CPF (a-c) pristine and (d-f) after 50 cycles.

In the pristine state, carbon black is uniformly distributed in the polyethylene film with a dense surface. After 50 cycles, the morphology nearly kept intact without any obvious corrosive damage, exhibiting excellent corrosion resistance and electrochemical stability of CPF.
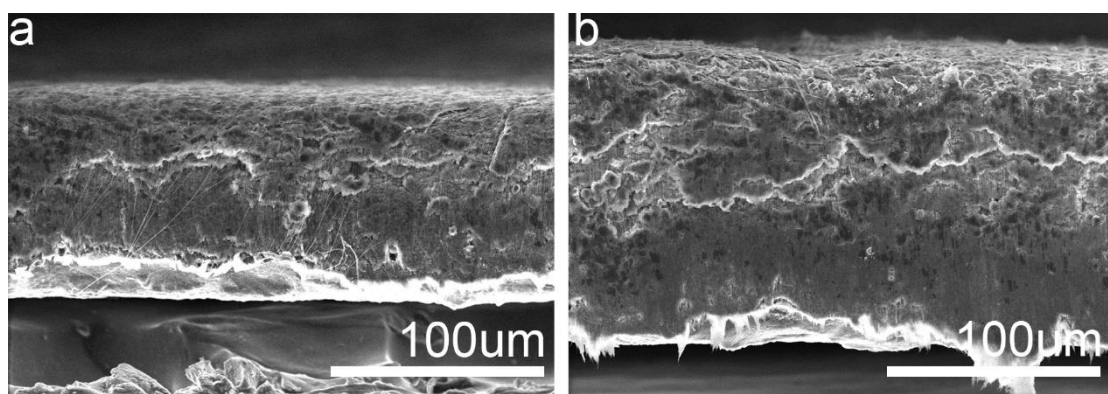
Figure S9. Cross section of KS6L/CPF cathode (a) pristine and (b) after 50 cycles.

In the pristine KS6L/CPF cathode, KS6L is tightly connected to the CPF. After 50 cycles, significant volume expansion can be observed on the KS6L while the contact between KS6L and CPF still maintains well.
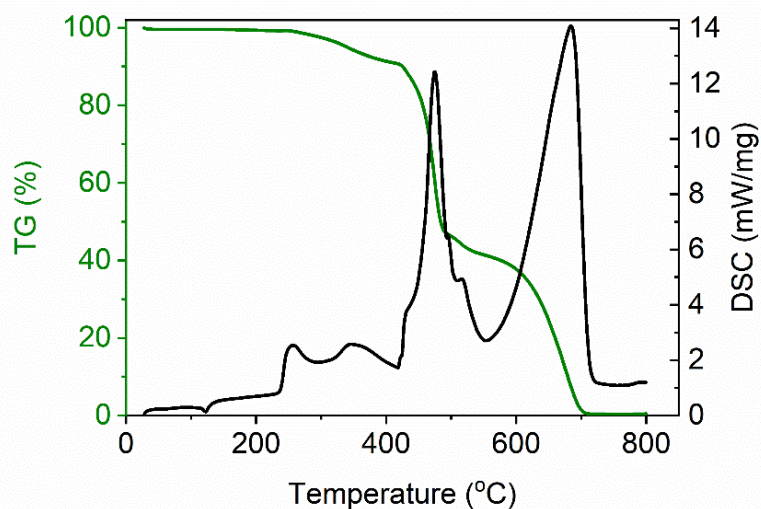
Figure S10. Thermo gravimetric (TG) and differential scanning calorimetry (DSC) curves of CPF at a heating rate of 10 ℃ /min from 25 to 800 ℃ under the air atmosphere.

Both DSC and TG curves remain stable until 240 ℃, though a small endothermic peak can be observed at 123 ℃ in DSC curves, indicating that CPF is stable, which is benefitial to the sealing process of B-RAB and meets the temperature requirements of wearable devices.
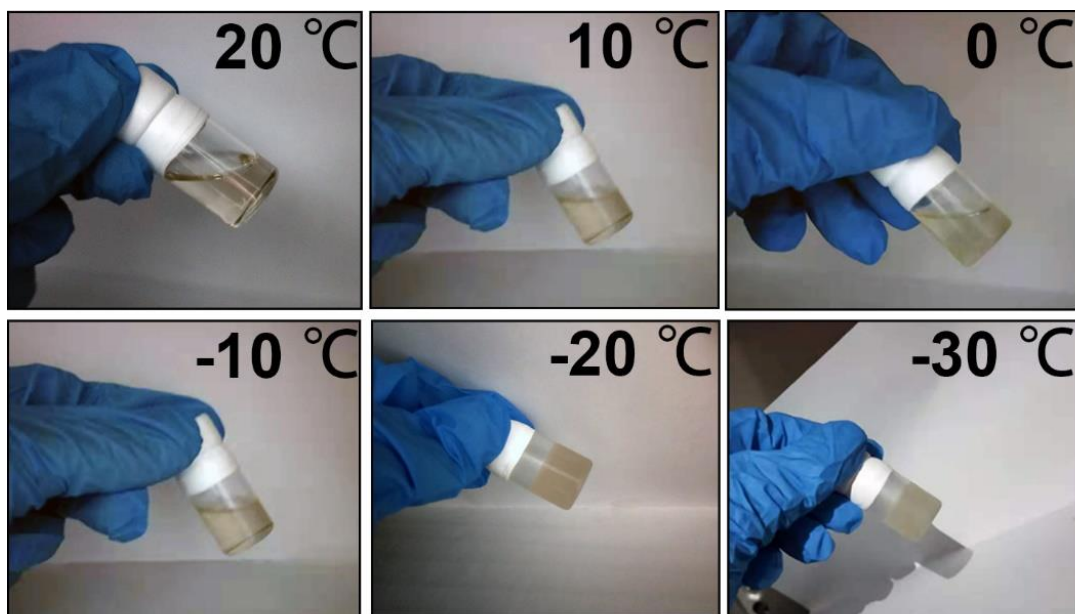
Figure S11. The optical pictures of the status of AlCl$_3$: [EMIm]Cl electrolyte from - 30 to + 20 °C.

The liquid AlCl$_3$: [EMIm]Cl electrolyte changes into solid when the temperature decreased from room temperature to -20 °C.
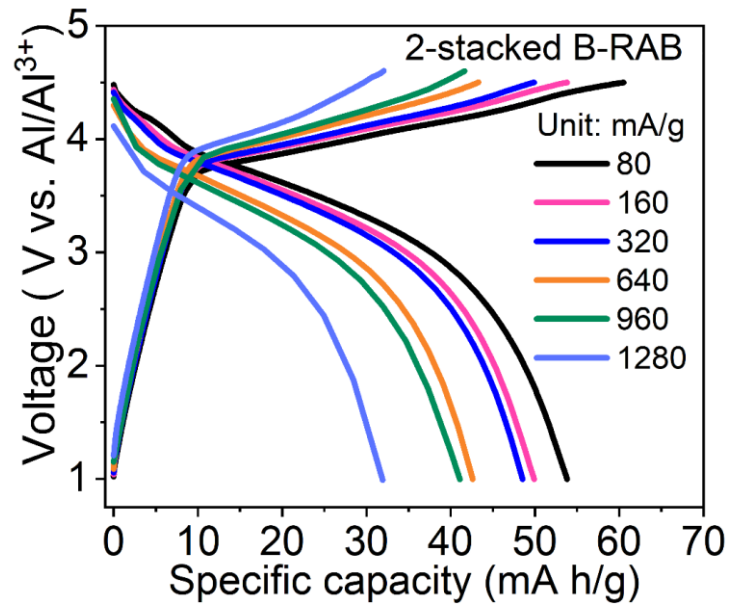
Figure S12. Charge and discharge curves of 2-stacked B-RAB at varied current densities from 80 to 1280 mAh/g.

As the current density increased to 960 mA/g, 2-stacked B-RAB could continuously provide a discharge capacity of above 40 mAh/g with small polarization, demonstrating the advantage of bipolar structure design on reducing ohmic loss and the great tolerance for the conductivity of current collectors.
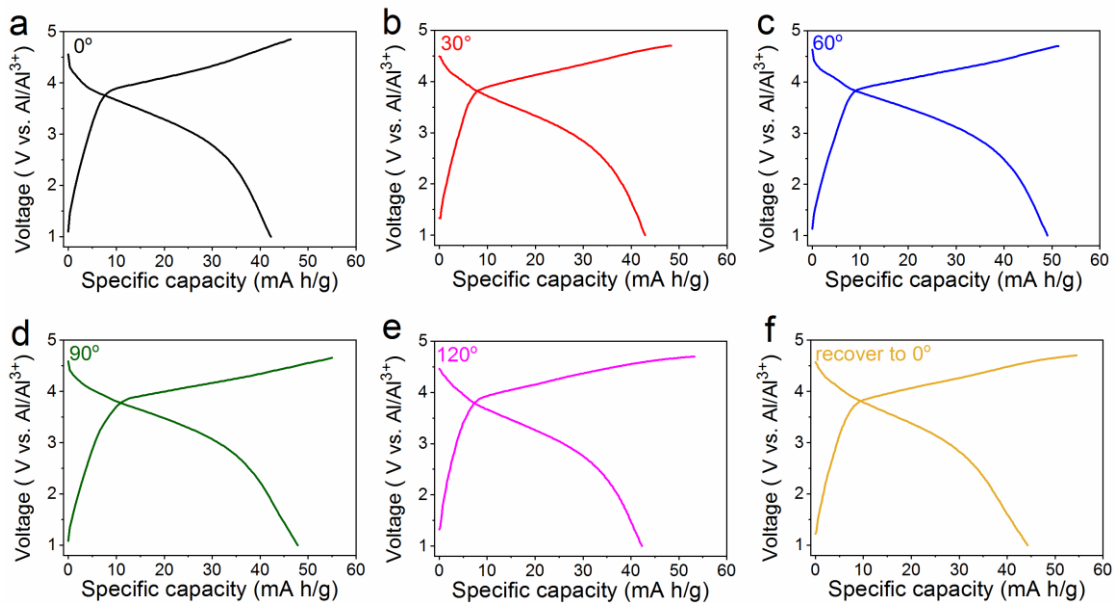
Figure S13. Charge and discharge curves of 2-stacked B-RAB at varied bending angles from 0° to 120°.

As the bending angle increases from 0° to 120° and recovers to 0°, 2-stacked B-RAB exhibits similar charge-discharge curves with a discharge capacity of above 40 mAh/g, demonstrating the favorable flexibility of B-RAB. A slight increase in capacity can be observed at 60°, which may be due to 1) the pouch cell might be under higher pressure; 2) after the initial activation process in a series of testing, there might be a gradual climb of capacity.
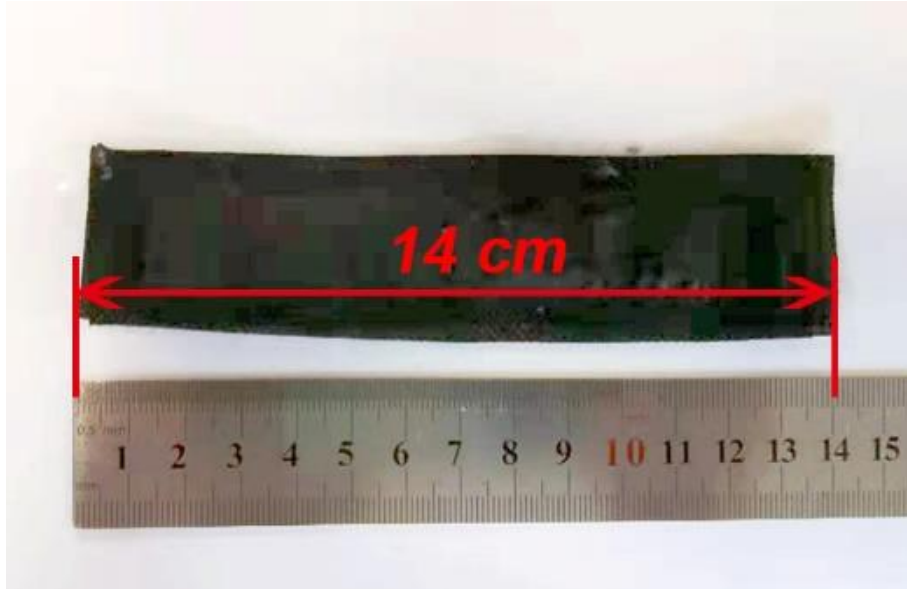
Figure S14. The optical picture and the length of 2-stacked B-RAB acting as the wearable watch strap.

Benefiting from the simple heat-sealed fabrication and good processability of CPF, the divers shape of battery can be produced according to application requirements.
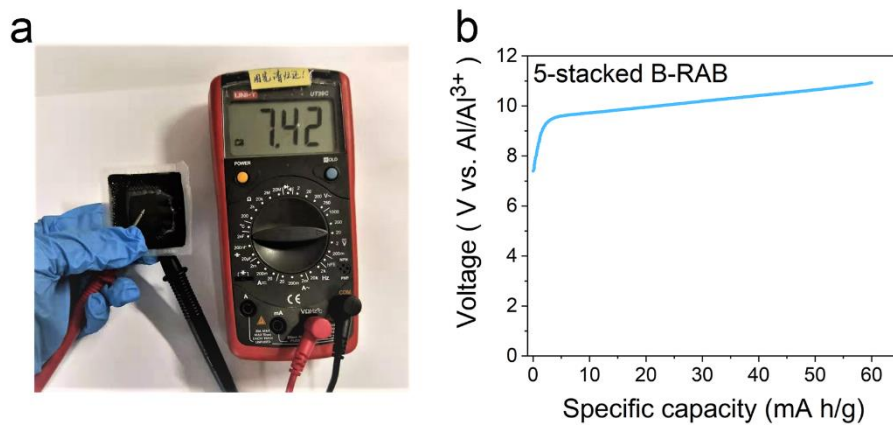
Figure S15. (a) Open circuit voltage of 5-stacked B-RAB, and (b) corresponding initial charge curve to 11V.

References

[1] Evanko, B.; Yoo, S. J.; Lipton, J.; Chun, S. E.; Moskovits, M.; Ji, X. L.; Boettcher, S. W.; Stucky, G. D. Stackable bipolar pouch cells with corrosion-resistant current collectors enable high-power aqueouselectrochemical energy storage. *Energy Environ. Sci.* **2018**, *11*, 2865−2875.

[2] D. Muñoz-Torrero, M. Anderson, J. Palma, R. Marcilla, E. Ventosa, Unexpected Contribution of Current Collector to the Cost of Rechargeable Al-Ion Batteries. *ChemElectroChem* **2019**, *6*, 2766-2770.